Diabatic processes and the winter North Atlantic Oscillation

Richard J. Greatbatch[1] and Thomas Jung[2]

[1] Department of Oceanography, Dalhousie University, Halifax, NS, Canada

[2] European Centre for Medium-Range Weather Forecasts, Reading UK

Submitted to Journal of Climate

Corresponding author address:

Dr. Richard Greatbatch, Department of Oceanography, Dalhousie University,

Halifax, Nova Scotia, Canada, B3H 4J1.

Email: richard.greatbatch@dal.ca

Short title: DIABATIC PROCESSES AND THE NAO

Abstract.

A version of the ECMWF operational model is used to diagnose and assess the importance of diabatic processes in the dynamics of the winter North Atlantic Oscillation (NAO). It is found that the diabatic forcing associated with the NAO in the model is dominated by the latent heat release associated with precipitation above the planetary boundary layer, and vertical diffusion, associated with the sensible heat flux from the ocean, within the boundary layer itself. To assess the feedback from the diabatic forcing on the NAO, model experiments have been conducted in which the diabatic forcing diagnosed from a control run is applied as a constant forcing in the model temperature equation. In the case of the positive NAO, the model response over the North Atlantic sector is dominated by the forcing from NAO-related diabatic heating over the North Atlantic itself, and acts as a significant, negative feedback. In the case of the negative NAO, the model response is dominated by the contribution from the tropics, indicating that warm El-Nino-like conditions in the tropical Pacific act as a forcing for the negative NAO in the model. The association between the negative NAO and warm conditions in the tropical Pacific is consistent with the composite analysis of Fraedrich and Müller. By contrast, we do not find evidence for a dynamical connection between cold conditions in the tropical Pacific and the positive NAO.

1. Introduction

As pointed out by Hoskins and Valdes (1990), a common observation in the atmosphere is that successive storms often follow the same track. Indeed, in the northern hemisphere winter, there are well-defined storm tracks that originate near the western boundary of the North Atlantic and North Pacific Oceans and extend eastwards across the ocean interior. This appears to contradict the notion that storms release available potential energy, reducing the local baroclinicity, and requiring the baroclinicity to be re-established before further storms can track in the same location. By looking at the dynamical response of a linear, stationary wave model to specified forcings computed from observations, Hoskins and Valdes concluded that the release of latent heat within the storm track provides a diabatic forcing for the atmosphere that feeds back to maintain the baroclinicity of the storm track. In this sense, the storm tracks are described as being "self-sustaining". In particular, the baroclinic zone on which the storm track depends is maintained by the dynamical response of the atmosphere to the diabatic heating that results from the storm track itself.

Hoskins and Valdes' work raises a question as to whether the same mechanism operates to self-maintain the modes of low frequency variability within the atmospheric circulation that are related to shifts in the positions of the storm tracks. Over the Euro-Atlantic sector, the most important mode of low frequency variability is the North Atlantic Oscillation (NAO). The NAO accounts for as much as 40 % of the variance in winter mean sea level pressure variability in that sector (see

Greatbatch (2000) and Hurrell et al. (2003) for reviews of the NAO). Winters of positive or negative NAO index are associated with displacements in the storm track over the North Atlantic (see, for example, Rogers, 1990). During negative NAO winters, the storm track is more zonally orientated near 40^oN, whereas in positive NAO winters, the storm track has a more southwest-northeast orientation. In this paper, we use a version of the ECMWF operational model to assess the role of diabatic forcing in the dynamics of the NAO. In particular, we are interested to know how the model responds to the diabatic heating associated with the positive and negative phases of the NAO and, in particular, whether the NAO-related diabatic forcing acts as a positive or a negative feedback on the NAO itself.

Evidence that the diabatic forcing acts as a positive feedback on the NAO has been put forward by Peterson et al. (2002) (see also Greatbatch et al. (2003)). These authors showed that a simple, dynamical model of the atmosphere has skill at reproducing the past history of the winter NAO index in the ensemble mean when driven by empirical forcing computed from observations, and attributed this skill to a positive feedback from the release of latent heat in the storm track (but see the discussion on this model in Section 4). Ting and Lau (1993), on the other hand, present evidence that the diabatic heating associated with the NAO acts as a negative feedback. These authors analyzed a 100 year experiment using an atmospheric general circulation model (AGCM) based on an EOF analysis of monthly means of 515 hPa height for the winter season defined as November to March, inclusive. The first EOF resembles the NAO in the model. Using a composite analysis, they identified the pattern of diabatic heating of the atmosphere associated with their first EOF. The local time tendency implied by the diabatic heating suggests a negative feedback, a conclusion reinforced when the diabatic heating was applied as a forcing for a model linearised about the winter mean state in the model. Evans and Black (2003) also find evidence that forcing associated with diabatic heating plays a role in both opposing the initial growth of weather regimes over the North Atlantic, and in assisting in their decay, again suggestive of a negative feedback.

Aside from the intrinsic interest as to whether the NAO-related diabatic heating of the atmosphere acts as a positive or negative feedback, it is important to understand the role of diabatic processes in the dynamics of the NAO in order to clarify how the ocean, and in particular sea surface temperature (SST) anomalies, influence the NAO (see, for example, Czaja et al., 2003). The issue of how SST anomalies influence the NAO is, in turn, an essential aspect of understanding the degree to which the NAO is predictable on seasonal and decadal time scales (e.g. Rodwell, 2003). Rodwell et al. (1999) showed that an AGCM driven by the observed time series of sea surface temperature (SST) and sea-ice at its lower boundary can reproduce, in the ensemble mean, the past history of the observed NAO index, at least on time scales longer than about 6 years. Other models also show this capability (e.g. Mehta et al., 2000; Latif et al., 2000). Rodwell et al. also showed that their model (the Hadley Centre AM2 model) exhibits an NAO response to the SST pattern forced by the NAO over the North Atlantic Ocean consistent with a positive feedback from the NAO-driven SST anomalies. The influence of SST anomalies on the NAO is ultimately attributable to diabatic forcing of the atmosphere induced by the SST anomalies. In the tropics, simple linear models have proved valuable tools for understanding the dynamical response of the atmosphere to diabatic heating sources (e.g. Gill, 1980). In the extratropics, the problem is much more complex, involving nonlinear interaction and feedback between the diabatic forcing and the transient eddy field, i.e. the storm track (Kushnir et al., 2002; Li and Conil, 2003).

Following discussion of the model and the experimental set-up in Section 2, we begin in Section 3 by describing the heat budget of the atmosphere associated with the NAO in the model. We then go on to describe the result of applying the diagnosed diabatic heating associated with the NAO as a forcing to the model, in order to ascertain, for example, the nature of the feedback between the diabatic heating released in the storm track and the NAO. The results are summarized in Section 4, where we also discuss some of the implications of our results.

2. Methods

The model used in this study is one of the latest versions of the ECMWF model (cycle 28rl) and was used operationally from 9 March to 27 September 2004. In this study a horizontal resolution of T_L95 (linear Gaussian grid $\approx 1.875^o$) is used and 60 levels in the vertical are employed. About half of the levels are located above the tropopause. The highest model level is located at about 0.1 hPa. Some aspects of the model performance at this resolution, including the stratosphere, are discussed in Jung and Tompkins (2003) and Jung (2005).

The model was first integrated for 6 months for each of the years from 1980 to 2001. Observed SST fields were used at the lower boundary, and the model was started on 1 October of each year. We call this set of model runs the "control" integration. Additional model runs are also conducted (see Section 4) in which diabatic forcing associated with the NAO, and diagnosed from the control run, is added as an extra, time-independent forcing to the model temperature equation, and the integration procedure repeated (that is, 22, 6 month integrations for each year from 1980 to 2001). Only the months from December through March are used for the subsequent diagnosis. The fact that the first two months of the integrations have been discarded ensures that the focus is on the winter season and that the model has reached its own climatology (see Jung, 2005). Subsequent results are based on monthly mean fields (a total of 88 fields).

The focus of this study is the diabatic forcing for the local temperature tendency in the model, in particular, that part of the forcing associated with the NAO. The *diabatic* processes simulated by the ECMWF model encompass radiative heating, vertical diffusion, gravity wave drag, as well as convective and large-scale precipitation. (Gravity wave drag plays no role in what follows, and will not be discussed further.) In the following, we shall refer to the total heating from precipitation, rather than the convective and large-scale contributions separately. It should be noted that precipitation heating refers to the latent heat release associated with condensation, and so can be expected to play a role in the storm track, and also in the tropics where there is deep convection. Likewise, in the planetary boundary layer, vertical diffusion includes the heating of the atmosphere due to the sensible heat flux from the ocean. The *adiabatic* forcing for the local temperature tendency accounts for horizontal and vertical advection as well as adiabatic effects due to vertical motion. We shall find that on the time scales considered here, the total diabatic and total adiabatic temperature forcings show a large cancellation, implying a negligible role for heat storage in the atmosphere, as one would expect.

The variability associated with the NAO (including the diabatic forcing associated with the NAO), is identified by means of a composite analysis. To characterize temporal variations of the NAO, we use a monthly NAO index defined, following Walker (1924), as the difference between the normalized monthly-mean sea-level pressure (SLP) time series from the grid points closest to the Azores and Iceland. We then composited monthly means of model variables whenever the model monthly NAO-index is greater than one standard deviation positive, or less than one standard deviation negative.

3. Results

3.1 The North Atlantic Oscillation

To verify the character of the NAO in the model, we first produced composites of monthly anomalies of 500 hPa height (Z500) and sea level pressure (SLP) for the winter months (December-March) for both the positive and negative NAO-index (as discussed above). The results (Figure 1) show the characteristic tendency for 500 and 1000 hPa height to both be lower (higher) than normal near Iceland in high (low) index years, with correspondingly higher (lower) than normal values near the Azores. Both the magnitude and pattern of the high and low index composites compare well with observed estimates (e.g. Anderson et al., 2003). Interestingly, the positive and negative composites are not the mirror image of each other, suggesting there may be some difference in the dynamics of the different phases of the NAO in the model (as issue we shall return to). Figure 1e,f show high and low index composites based on monthly mean anomalies in the standard deviation of day-to-day changes in 500 hPa heights (see Jung 2005, for details about the characteristics of this highpass-filter), indicating the displacement in the storm track between high and low index months. Again we see the characteristic tendency for a strengthened (weakened) storm track from Newfoundland to the Norwegian Sea in high (low) index months with bands of weakened (increased) storm activity to the north and south, much as in the observations.

3.2 Heat budget

We now turn to the forcing for the local temperature tendency in the ECMWF model. Figure 2 shows this forcing, zonally-averaged over the North Atlantic region (100^{o}W–20^{o}E). The winter climatological forcing is shown using contours and the difference between high and low NAO index composites is shown using shading. For both the climatology and the high minus low index composites, we see that there is a cancellation between the total diabatic and abiabatic temperature forcing, indicating, as noted earlier, that there is no significant role for heat storage in the atmosphere on the time scales (monthly-mean and longer) studied here. Not surprisingly, the radiative forcing has a role to play in the climatological forcing balance, the net effect being a radiative heat loss to space everywhere outside the near surface zone. The impact of latent heating associated with precipitation is evident in the equatorial region (deep convection) and the midlatitude storm track centred near 40^oN (see also Hantel and Baader, 1978). In the high minus low NAO index composite, the radiative forcing plays only a minor role. Above the boundary layer, the NAO-related diabatic forcing is dominated by the contribution from precipitation (i.e. latent heat release), with little or no contribution from vertical diffusion (e.g. sensible heat flux from the ocean). By contrast, within the boundary layer, vertical diffusion (i.e. sensible heat flux from the ocean) plays the dominant role and has the same sign as the heating anomalies due to precipitation above the boundary layer in the same latitude band. Both the sensible heat flux anomalies, and the precipitation heating anomalies are, themselves, associated with the NAO-related shifts in the storm track noted in Figure 1e,f. Note, in particular, that, in the high NAO-index state, there are enhanced surface westerly winds in the band from 45^o N to 65^o N (Figure 1c) that are associated with both enhanced heat flux and evaporation from the ocean (Figure 2d; see, also, Cayan, 1992), and with enhanced latent heat release (Figure 2f) associated with the storm track (Figure 1e). Interestingly, within the boundary layer, the anomalous heat flux from the ocean counters opposite signed anomalies associated with precipitation that are, themselves, of opposite sign to the precipitation anomalies above the boundary layer. The change in sign of the anomalous precipitation heating at the top of the boundary layer is because of cooling due to evaporation of precipitation within the boundary layer itself.

The above conclusions are further clarified by the horizontal plan views shown in Figures 3 and 4 at two different levels, roughly 960 hPa and 540 hPa, respectively.

Again, at both levels, we see the balance between the net diabatic and adiabatic temperature forcing. The role of the vertical diffusion (in particular, sensible heat flux from the ocean) is clearly evident in the boundary layer (Figure 3d), where, as before, the sign of the total diabatic heating is determined by the vertical diffusion, but plays virtually no role above (Figure 4d). At 540 hPa, on the other hand, the difference composite is dominated by the contribution from the precipitation, with the radiative forcing, as noted previously, having only a minor role to play. An interesting feature in Figures 3 and 4 is that heating anomalies associated with precipitation are often found upstream of heating anomalies of the same sign due to vertical diffusion (predominently heat flux from the ocean). A good example is the region of heat gain over the Labrador Sea in the high-minus-low index composite shown in Figure 3, and the corresponding region of precipitation heating in a band further east, north of the British Isles, in Figure 4. As noted earlier, the enhanced (reduced) sensible heat loss over the Labrador Sea associated with the positive (negative) NAO is also associated with enhanced (reduced) evaporation, and hence anomalies in moisture input to the atmosphere that feed the corresponding precipitation heating anomalies.

3.3 Diabatically forced experiments

In the perturbed experiments, the sensitivity of the atmospheric circulation to a component of the NAO-related diabatic temperature forcing is studied by applying that component of the heating (diagnosed from the control run) as a time-independent forcing to the model temperature equation during the full cycle of integrations with the model (that is, throughout each of the 6 month integrations for each year from 1980 to 2001). In particular, the model equations become

$$\frac{d\mathbf{x}_t}{dt} = G(\mathbf{x}_t) + \mathbf{F}_{NAO} \tag{1}$$

where $\mathbf{x}_t$ describes the time-dependent atmospheric state vector, G symbolizes the dynamical and physical part of the ECMWF model, and $\mathbf{F}_{NAO}$ is the time-independent NAO-related forcing that is non-zero for the temperature equation only. For the positive (negative) NAO cases shown below, the forcing $\mathbf{F}_{NAO}$ is the positive (negative) NAO composite diagnosed from the control run.

Figure 5 shows the difference between the mean fields (perturbed experiments minus control) for Z500 and Z1000 when the forcing in the perturbed case is the global, total diabatic forcing associated with the positive (Fig. 5a,c) and the negative (Fig. 5b,d) NAO. In the positive NAO case, the model response at 500 hPa projects on to the NAO pattern (Figure 1a), but with the sign reversed, indicating that the total, global diabatic forcing associated with the positive NAO excites a negative NAO response. Comparing Figure 1a and 5a, we see that the magnitude of the forced response in the positive NAO case amounts to about 30–40% to that of the canonical NAO in the model, indicating a strong signal. However, there is a tendency for the model response to be south-eastward shifted compared to the standard NAO pattern (Figure 1), particularly for the Icelandic low centre. At the surface (Fig. 5c) the response shows little resemblance with the NAO, and in the negative NAO case (Figure 5b,d), the model response more closely resembles a wave train emanating from the tropical Pacific than a response to the local diabatic heating.

The suggestion of remote, tropical forcing in the negative NAO case (an issue to be explored further when we discuss Figure 11) indicates the need to separate the diabatic forcing over the North Atlantic sector (the part of the forcing most likely to be driven by the NAO itself) from the remote forcing (which is likely to arise from factors not directly related to the NAO).

We have also computed probability density functions (pdf's; see Figure 6) of monthly mean differences in Z1000 and Z500 between the Azores and Iceland (proxies for the NAO index). The pdf's shown in Figure 6a,f confirm the conclusions above. In particular, in the positive NAO case (dotted line), the pdf is slightly shifted leftward at 500 hPa compared to the control run (solid line), but with little change in the pdf at 1000 hPa. In the negative NAO-case, the pdf suggests a substantial negative NAO response which, as we shall see later, is associated with forcing from the tropical Pacific.

Figure 7 shows the corresponding model results when the total diabatic forcing associated with the NAO is restricted to the North Atlantic sector only. This time (see also the pdf's in Figure 6b,g), the model shows an NAO-response at 500 hPa that is of the opposite sign to that associated with the forcing in both the positive and negative NAO cases. Since the forcing in this case is a strong function of the NAO itself, these results indicate that the diabatic feedback for the NAO in the model is negative. Although the magnitude of the feedback is greater in the positive NAO case, the model response is significantly different from zero at the 95 % level for both positive and negative NAO forcing. At the surface the response is less clear. A comparison between Figure 5a,c and 7a,c reveals that the negative NAO response found at 500 hPa when using the global diabatic forcing for the positive phase of the NAO is primarily due to diabatic processes local to the North Atlantic. Indeed, the model response over the Euro-Atlantic sector in Figure 7a,c is quite similar to that in Figure 5a,c. In the negative NAO case, on the other hand, it seems that diabatic processes outside of the North Atlantic region are needed to explain the response shown in Figure 5b,d (see below).

We can go further and split the model forcing (see Section 2) into that part associated with vertical diffusion (primarily sensible heat flux from the ocean; Figure 8), and that part associated with precipitation (latent heat release in the storm track; Figure 9). In the former (Figure 8), a negative feedback is still apparent in the positive NAO cases, while the model response in the negative NAO cases shows no projection onto the NAO pattern (see also the pdf's shown in Figure 6c,h, and note that in the negative NAO case forced by vertical diffusion, the pdf at 500 hPa almost completely overlays the control case). When forcing by precipitation heating associated with the positive NAO (Figure 9a,c), the model response at 500 hPa shows a statistically significant (at the 95 % level), southeastward-shifted, negative NAO pattern with magnitude about 30% that of the canonical NAO, again indicating a negative feedback (also evident from the pdf; the dotted curve in Figure 6i). On the other hand, with negative NAO forcing (Figure 9c,d), there is effectively no response at 500 hPa, but the indication of a westward-shifted negative NAO response (i.e. a positive feedback) at 1000 hPa that is also significantly different from zero at the 95 % level. We can summarise the above results by saying that the model response to diabatic forcing associated with the positive NAO shows a clear negative feedback from the local diabatic heat release over the North Atlantic sector, with contributions from both vertical diffusion (heat transfer from the ocean) and precipitation heating, but that the feedback is weaker and less coherent in the negative NAO case.

3.4 Forcing from the tropical Pacific

As is evident by comparing Figures 5 and 7, the model response to NAO-related diabatic heating has a large signal originating outside of the North Atlantic region. In fact, in the negative NAO case, the remotely-forced signal dominates the local, North Atlantic forced response. Figure 10 shows the diabatic temperature forcing for the model integrated from 850–200 hPa for the control run (Figure 10a), and the anomalous heating that goes along with the negative (Figure 10b) and positive (Figure 10c) NAO. By focussing on the free troposphere the diabatic forcing is dominated by the release of latent heat (i.e., precipitation). The anomalous heating in the negative NAO case is clearly indicative of El Nino (warm) conditions in the central tropical Pacific, whereas the positive NAO case corresponds to La Nina (cold) conditions.

In order to investigate the role of tropical forcing on the monthly mean NAO, two additional experiments have been carried out, one in which the precipitation forcing, restricted to the tropical Pacific (20^oS–20^oN and 100^oW–100^oE), is associated with the negative and one with the positive NAO (see Fig. 10b,c). The model response for both the positive and negative NAO cases shows what looks like a wave train that originates over the tropical Pacific (Figure 11). There are, however, important differences between the two wave trains. In particular, the wave train in the negative NAO case (associated with El Nino-like conditions in the tropical Pacific) is much stronger, particularly in the North Pacific basin, and seems to originate further to the east than the wave train associated with the positive NAO forcing (La Nina-like conditions in the tropical Pacific). Furthermore, over the North Atlantic itself, the impact is weak in the positive NAO case, but much stronger in the negative NAO case. These conclusions are confirmed by Figure 12 which shows the difference in the mean 200 hPa divergent wind and Rossby wave source (following equation (3) in Sardeshmukh and Hoskins (1988)) between each of the negative and positive NAO-forced cases and the control run. These figures show a strong Rossby wave source associated with an anomalous outflow from the central tropical Pacific in the case of the negative NAO (Figure 12b) (as one would expect in an El Nino situation), compared to an anomalous inflow that is shifted to the west in the positive NAO case (Figure 12c) (the negative NAO case - Figure 12b - also indicates a Rossby wave source over the Gulf of Mexico). The weakness of the Euro-Atlantic response to tropical forcing in the positive NAO case is consistent with our previous finding that the tropical forcing is less important in that case; rather the model response is dominated by the local diabatic (negative feedback). By contrast, in the negative NAO case, tropical forcing is the dominent diabatic forcing, and furthermore, forces a negative (same sign) response over the North Atlantic. (Note that this does not indicate a positive feedback because the tropical forcing is not likely to be forced by the NAO itself, but, rather by other processes external to the NAO.) The pdf's shown in Figure 6 nicely summarise these results.

In the case of precipitation forcing from the tropical Pacific associated with the negative NAO, the pdf in Figure 6e,j is noticably shifted to the left compared to the control run, indicating a negative NAO response on average, whereas under forcing associated with the positive NAO, there is effectively no shift in the pdf.

Hoerling et al. (1997) have noted that the mid-latitude teleconnection associated with El Nino versus La Nina events is not linear, and, in fact, has features in common with our results, at least over North America. They attribute the nonlinearity to an asymmetry in the anomalous forcing in the tropics associated with precipitation. It should be noted that the association between the negative (positive) NAO and warm (cold) events in the central tropical Pacific is broadly consistent with the data study of Fraedrich and Müller (1992), and with the modelling studies of Merkel and Latif(2002), Mathieu et al. (2004), and Pohlmann and Latif (2005). Brönnimann et al. (2004) have also suggested a persistent El Nino, with an atmospheric teleconnection pattern similar to our negative NAO case, as an explanation for the major climate anomaly of 1940/42, particularly the exceptionally cold winter of 1941/42 in European Russia.

The reader might be surprised finding that La Nina-like conditions dominate for positive NAO months in the ECMWF model (Figure 10c), despite the fact that the experiment with the La Nina-type heating imposed does not show any significant response in the North Atlantic region (Figure 11a,c). In order to understand this apparent contradiction, suppose that the only link between the tropical Pacific and the North Atlantic is between El Nino-like conditions and the negative NAO (as suggested by this study). In this case the composite for positive NAO months will be biased towards La Nina cases giving rise to a spurious link between the two phenomena. This shows that numerical experimentation, such as carried out in this study, is crucial for understanding the nature of the link between the tropical Pacific and the North Atlantic.

4. Summary and discussion

We began Section 3 by using a composite analysis to describe the diabatic forcing for the local temperature tendency that is associated with the NAO in the ECMWF model. Above the planetary boundary layer, we found that the diabatic forcing associated with the NAO is dominated by the latent heat release due to precipitation (that is, convection plus large scale), whereas in the boundary layer itself, the diabatic forcing is dominated by vertical diffusion (in particular, the sensible heat flux from the ocean). We found that heating anomalies associated with precipitation tend to occur downstream of anomalies of the same sign in heat flux (and evaporation) from the ocean, suggesting that the latter feed the former. Both sets of anomalies also shift with the NAO so that there is enhanced (reduced) heat loss from the ocean where the westerly winds are strengthed (weakened) and corresponding enhanced (reduced) precipitation heating where the storm track is strengthed (weakened).

To understand the feedback from the diabatic forcing, we described experiments in which the diabatic forcing associated with the NAO, and diagnosed from the control run, is applied as an additional, time-independent forcing to the temperature equation in the ECMWF model. The results indicate that for the positive NAO, the diabatic forcing acts as a negative feedback, and is predominently a response to NAO-forced diabatic heating over the North Atlantic itself, indicating a genuine negative feedback. In the case of the negative NAO, the model response is dominated by a forced response from the tropics in association with warm, El Nino-like conditions in the tropical Pacific. The negative feedback in the positive NAO case (and which can also been seen in the negative NAO case when the forcing is restricted to the North Atlantic sector only) is consistent with the negative feedback from diabatic forcing found by Ting and Lau (1993) for an NAO-like mode in an AGCM, and also with the general tendency for diabatic heating to act as a negative (if weak) feedback on Atlantic weather regimes (Evans and Black, 2003).

The starting point for the work presented here was the conclusion reached by Hoskins and Valdes (1990) that the latent and sensible heating associated with the climatological storm track acts as a positive feedback such as to "self-sustain" the climatological storm track. We noted in the introduction that the variability of the NAO is associated with major shifts of the storm track (e.g. Rogers, 1990), and the question arose as to whether the mechanism identified by Hoskins and Valdes (1990) acts to self-sustain the storm track in the different phases of the NAO. Our results show that in the ECMWF model, at least, this self-sustaining mechanism does not operate for the NAO, since the feedback from the diabatic forcing associated with shifts in the storm track is negative (Figure 7). Despite these rather negative results concerning the role of the self-sustaining mechanism in the dynamics of the NAO, it should be remembered that latent heat release due to precipitation can be a potent force in amplifying middle latitude storms (Wernli and Davies 1997) and hence may play an indirect role in the dynamics of the NAO by modifying the eddy fluxes (particularly the eddy flux of westerly momentum) that are believed to be important in sustaining the different phases of the NAO (see Thompson et al., 2003).

Our results raise questions concerning the ability of the simple GCM used by Peterson et al. (2002) to reproduce, in an ensemble mean sense, the past time history of the winter NAO, and suggest that the success of their model is not because of a positive feedback from the diabatic forcing associated with the NAO, as suggested by these authors. A complication in their study is that the empirical forcing used to force the model does not apply simply to the temperature equation, but also to the equations for vorticity, divergence and surface pressure as well (see Greatbatch et al., 2003, for a discussion of the complications that can result from this). A particular weakness of the model is that it has a flat bottom, with the consequence that information about the presence of mountain ranges must also be present in the model forcing. Since the forcing associated with mountain ranges is flow-dependent, it is possible that the success of the Peterson et al. study in reproducing the time history of the observed NAO is not because of a positive feedback from the NAO-related diabatic heating, but rather is because the model uses a flat bottom.

A feature of our model results is the importance of the signal emanating from the tropical Pacific, particularly the evidence that in the model, the negative NAO is being forced by warm, El Nino-like conditions in the tropical Pacific. The association of the negative NAO with warm conditions in the tropical Pacific is broadly consistent with the composite analysis of Fraedrich and Müller (1992), and the modelling studies of Merkel and Latif (2002), Mathieu et al. (2004) and Pohlmann and Latif (2005). Nevertheless, it has been suggested that the impact of ENSO on the Euro-Atlantic sector is not robust, and might vary on interdecadal time scales (van Loon and Madden, 1981; Rogers, 1984; Greatbatch et al., 2004). Similarly, Lin et al. (2005) have argued for a connection between convection anomalies in the tropical Pacific and the positive NAO that does not appear to be consistent with our results. Given that much of the skill associated with seasonal prediction in believed to originate in the tropical Pacific (e.g. Stockdale, 2000; Derome et al., 2001), the nature of the teleconnection response between the tropical Pacific and the Euro-Atlantic sector is clearly a topic requiring further research.

Finally, the question of how and to what extent extratropical SST anomalies drive the atmosphere, and the NAO in particular, is still surrounded by controversy. As noted by Kushnir et al. (2002), the mechanism must involve interaction and feedback between the diabatic forcing of the atmosphere and the transient eddies, and the ability of the transient eddies to organize an equivalent barotropic, as distinct from a shallow, baroclinic, response (Li and Conil, 2003). As noted in the introduction, the influence of SST anomalies on the NAO must ultimately be attributable to diabatic forcing of the atmosphere induced by the SST anomalies. Since SST anomalies are expected to change the surface flux of heat and moisture from the ocean, one would expect heating associated with vertical diffusion and precipitation to play a role. It is instructive to extrapolate our model results for the positive NAO case (for which we saw a clear negative NAO response) to speculate about the atmospheric response to SST anomalies associated with the negative NAO; that is, warm anomalies in the subpolar gyre, between 45^o N and 65^o N, and cold anomalies immediately to the south and west (see Visbeck et al., 2003). If these anomalies modify the surface fluxes by the same sign, i.e. by increasing the surface heat and moisture flux from the ocean to the atmosphere over the subpolar gyre, and decreasing the flux further to the south, then because these changes in surface heat flux are of the same sign as diagnosed from our model in association with the positive NAO (see Figure 3d), our results suggest a negative NAO response. Such a response implies a positive feedback from the underlying SST anomalies on the negative NAO. Furthermore, the implied changes in surface heat flux, and the corresponding atmospheric response, are consistent with the numerical experiment described by Rodwell et al. 1999). Clearly, this is another topic that needs to be explored further in future work.

Acknowledgments

RJG receives support from the Canadian CLIVAR Research Network funded by NSERC and CFCAS, and the NSERC/MARTEC/MSC Industrial Research Chair. We are grateful to Holger Pohlmann for comments that led to improvements in the manuscript.

References

Anderson, D., T. Stockdale, M. Balmaseda, L. Ferranti, F. Vitart, F. Doblas-Reyes, R. Hagedorn, T. Jung, A. Vidard, A. Troccoli and T. Palmer, 2003: Comparison of the ECMWF seasonal forecasts System 1 and 2, including the relative performance for the 1997/8 El Nino. Technicial Report 404, ECMWF, Shinfield Park, Reading, Berkshire RG2 9AX, UK.

Brönnimann, S., J. Luterbacher, J. Staehelin, T.M. Svendby, G. Hansen and T. Svense, 2004: Extreme climate of the global troposphere and stratosphere in 1940-42 related to El Nino. *Nature*, **431**, 971–974.

Cayan, D.R., 1992: Latent and sensible heat flux anomalies over the northern oceans: driving the sea surface temperature. *J. Phys. Oceanogr.*, **22**, 859–881.

Czaja, A., A.W. Robertson and T. Huck. 2003: The role of Atlantic ocean-atmosphere coupling in affecting North Atlantic Oscillation variability. *The North Atlantic Oscillation*, J. Hurrell, Y. Kushnir, G. Ottersen and M. Visbeck, Eds., Geophysical Monograph Series, **134**, American Geophysical Union, 147–172.

Derome, J., G. Brunet, A. Plante, N. Gagnon, G. Boer, F. Zwiers, S. Lambert, J. Sheng and H. Ritchie, 2001: Seasonal predictions based on two dynamical models. *Atmos-Ocean*, **39**, 485–501.

Evans, K.J., and R.X. Black, 2003: Piecewise tendency diagnosis of weather regime transitions. *J. Atmos. Sci.*, **60**, 1941–1957.

Fraedrich, K., and K. Müller, 1992: Climate anomalies in Europe associated with ENSO extremes. *Int. J. Climatol.*, **12**, 25–31.

Gill, A.E., 1980: Some simple solutions for heat-induced tropical circulation. *Quart. J. Roy. Met. Soc.*, **106**, 447–462.

Greatbatch, R.J, 2000: The North Atlantic Oscillation. *Stochastic Environmental Research and Risk Assessment*, **14**, 213-242.

Greatbatch, R.J., H. Lin, J. Lu, K.A. Peterson and J. Derome, 2003: Tropical/Extratropical forcing of the AO/NAO: A corrigendum. *Geophys. Res. Lett*, **30**, 1738, doi:10.1029/2003GL017406.

Greatbatch, R.J., J. Lu and K.A. Peterson, 2004: Non-stationary impact of ENSO on Euro-Atlantic winter climate. *Geophys. Res. Lett.*, **31**, L02208, doi:10.1029/2003GL018542.

Hantel, M., and H.-R. Baader, 1978: Diabatic heating climatology of the zonal atmosphere. *J. Atmos. Sci.*, **35**, 1180–1189.

Hoerling, M.P., A. Kumar and M. Zhong, 1997: El Nino, La Nina, and the nonlinearity of their teleconnections. *J. Climate*, **10**, 1769-1786.

Hoskins, B.J., and P.J. Valdes, 1990: On the existence of storm tracks. *J. Atmos. Sci.*, **47**, 1854–1864.

Hurrell, J.W., Y. Kushnir, G. Ottersen, and M. Visbeck, 2003: An Overview of the North Atlantic Oscillation. *The North Atlantic Oscillation*, J. Hurrell, Y.

Kushnir, G. Ottersen and M. Visbeck, Eds., Geophysical Monograph Series, **134**, American Geophysical Union, 1–35.

Jung, T., 2005: Systematic errors of the atmospheric circulation in the ECMWF forecasting system. *Quart. J. Roy. Meteor. Soc.*, **131**, 1045–1073.

Jung, T., and A.M. Tompkins, 2003: Systematic errors in the ECMWF forecasting system. Technical Report 422, ECMWF, Shinfield Park, Reading, Berkshire RG2 9AX, UK.

Kushnir, Y., W.A. Robinson, L. Bladé, N.M.J. Hall, S. Peng and R. Sutton, 2002: Atmospheric GCM response to extratropical SST anomalies: synthesis and evaluation. *J. Climate*, **15**, 2233–2256.

Latif, M., K. Arpe and E. Roeckner, 2000: Oceanic control of decadal North Atlantic sea level pressure variability in winter. *Geophys. Res. Lett.*, **27**, 727–730.

Li, Z. X., and S. Conil, 2003: Transient response of an atmospheric GCM to North Atlantic SST anomalies. *J. Climate*, **16**, 3993–3998.

Lin, H., J. Derome and G. Brunet, 2005: Tropical Pacific link to the two dominant patterns of atmospheric variability, 32, L03801, doi:10.1029/2004GL021495.

Mathieu, P.-P., R.T. Sutton, B. Dong and M. Collins, 2004: Predictability of winter climate over the North Atlantic European region during ENSO events. *J. Climate*, **17**, 1953–2772.

Merkel, U., and M. Latif, 2002: A high resolution AGCM study of the El Nino impact on the North Atlantic/European sector. Geophys. Res. Lett., **29**, doi:10.1029/2001GL013726.

Mehta, V.M., M.J. Saurez, J. Manganello and T.L. Delworth, 2000: Ocean influence on the North Atlantic Oscillation and associated northern hemisphere climate variations. *Geophys. Res. Lett.*, **27**, 121–124.

Peterson, K.A., R.J. Greatbatch, J. Lu, H. Lin and J. Derome, 2002: Hindcasting the NAO using diabatic forcing of a simple AGCM, *Geophys. Res. Lett.*, **29**, 10.1029/2001GL014502.

Pohlmann, H., and M. Latif, 2005: Atlantic versus Indo-Pacific influence on Atlantic-European climate. *Geophys. Res. Lett.*, **32**, L05707, doi:10.1029/2004GL021316.

Rodwell, M.J. 2003: On the predictability of North Atlantic climate. *The North Atlantic Oscillation*, J. Hurrell, Y. Kushnir, G. Ottersen and M. Visbeck, Eds., Geophysical Monograph Series, **134**, American Geophysical Union, 173–192.

Rodwell, M.J., D. P. Rowell, and C. K. Folland, 1999: Oceanic forcing of the wintertime North Atlantic Oscillation and European climate. *Nature,* **398**, 320–323.

Rogers, J.C., 1984: The association between the North Atlantic Oscillation and the Southern Oscillation in the northern hemisphere. *Mon. Wea. Rev.*, **112**, 1999–2015.

Rogers, J.C., 1990: Patterns of low frequency monthly sea level variability

(1899-1986) and associated wave cyclone frequencies. *J. Climate*, **3**, 1364–1379.

Sardeshmukh, P., and B.J. Hoskins, 1988: The generation of global rotational flow by steady, idealised tropical divergence. *J. Atmos. Sci.*, **45**, 1228–1251.

Stockdale, T., 2000: An overview of techniques for seasonal forecasting. *Stochastic Environmental Research and Risk Assessment*, **14**, 305–318.

Thompson, D.W.J., S. Lee and M.P. Baldwin. 2003: Atmospheric processes governing the Northern hemisphere Annular Mode/North Atlantic Oscillation. *The North Atlantic Oscillation*, J. Hurrell, Y. Kushnir, G. Ottersen and M. Visbeck, Eds., Geophysical Monograph Series, **134**, American Geophysical Union, 81–112.

Ting, M., and N.-C. Lau, 1993: A diagnostic and modeling study of the monthly mean wintertime anomalies appearing in a 100-year GCM experiment. *J. Atmos. Sci.*, **50**, 2845–2867.

van Loon, H., and R.A. Madden, 1981: The Southern Oscillation. Part I: Global associations with pressure and temperature in northern hemisphere winter. *Mon. Wea. Rev.*, **109**, 1150–1162.

Visbeck, M., E.P. Chassignet, R.G. Curry, T.L. Delworth, R.R. Dickson and G. Krahmann, 2003: The ocean's response to North Atlantic Oscillation variability. *The North Atlantic Oscillation*, J. Hurrell, Y. Kushnir, G. Ottersen and M. Visbeck, Eds., Geophysical Monograph Series, **134**, American Geophysical Union, 113–146.

Walker, G.T., 1924: Correlation in seasonal variation of weather, IX. *Mem. Indian. Meteor. Dep.,* 24, 275–332.

Wernli, H., and H.C. Davies, 1997: A Lagrangian-based analysis of extratropical cyclones. I: The method and some applications. *Quart. J. Roy. Meteor. Soc.,* 123, 467–489.

Received ; revised ; accepted .

List of Figures

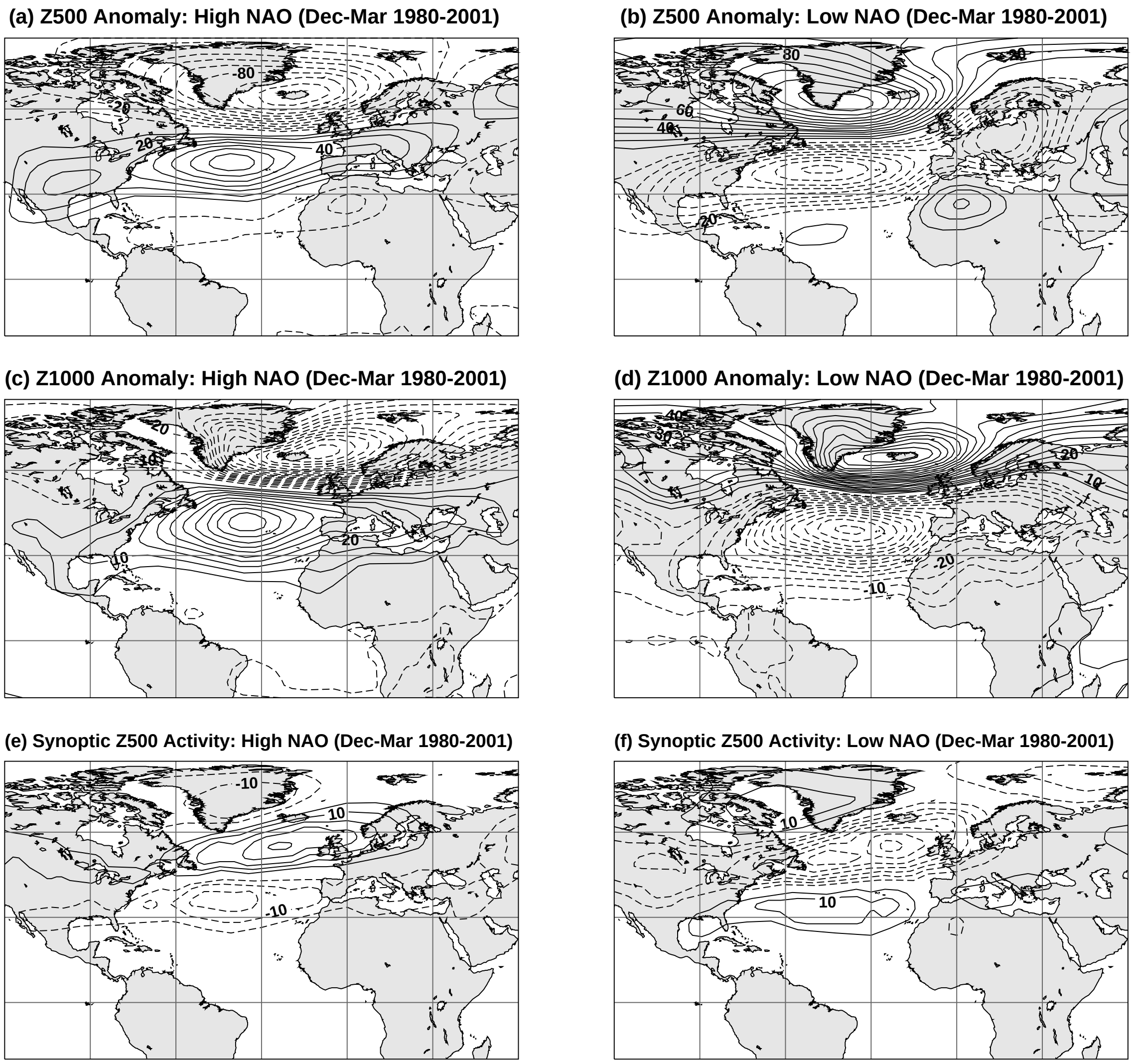

Figure 1. Monthly mean anomalies associated with the high and low phase of the NAO during winter months of the period 1980–2001 for the ECMWF model: (a)–(b) 500 hPa geopotential height (contour interval is $10m$), (c)–(d) 1000 hPa geopotential height (contour interval is $5m$), and (e)–(f) synoptic Z500 activity (contour interval is $5m\,d^{-1}$). (a), (c) and (e) represent high and (b), (d) and (f) low NAO conditions. A threshold of plus (minus) one standard deviation of the monthly NAO index has been used for compositing. Shown are differences between the composites and long term means. Synoptic Z500 activity is defined as the standard deviation of day-to-day Z500 changes.

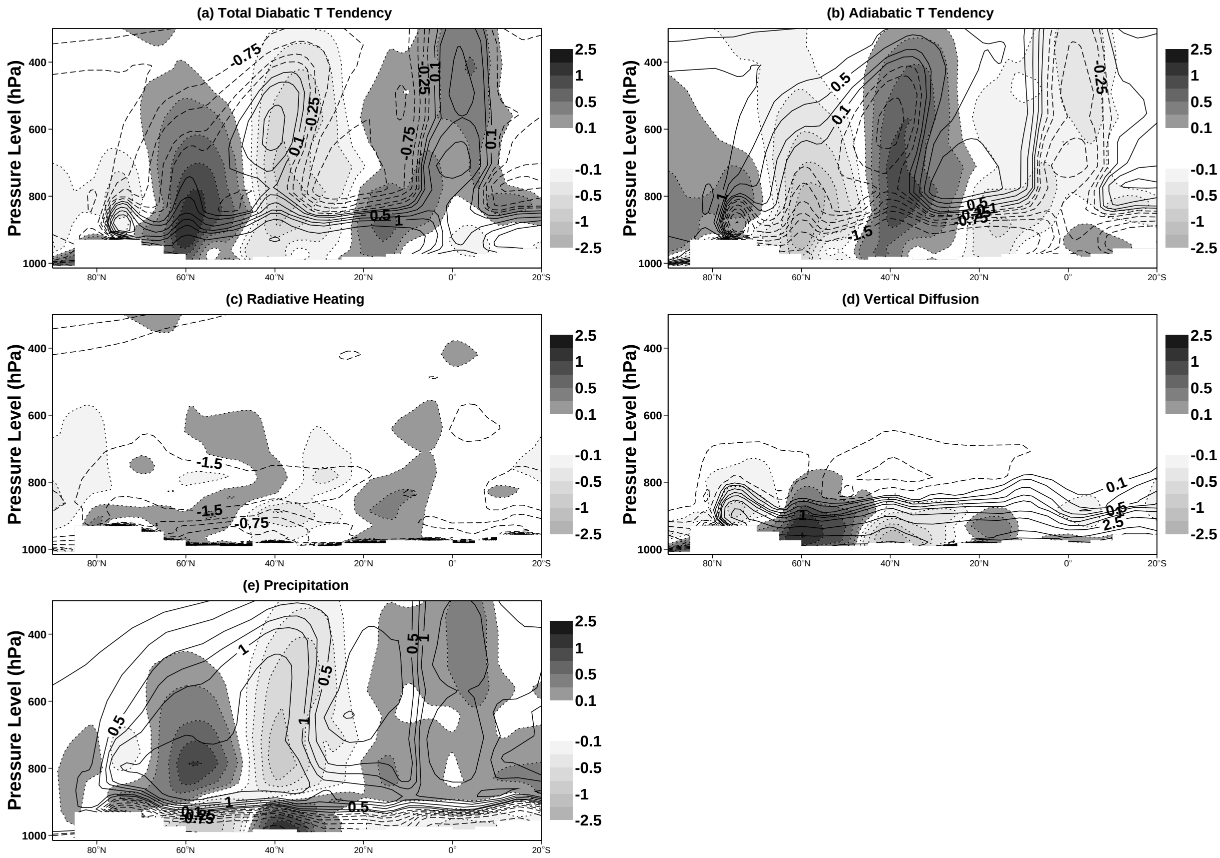

Figure 2. Zonal average of the temperature forcing ($K\ day^{-1}$) over the North Atlantic region (100^{o}W-20^{o}E) for the ECMWF model: (a) total diabatic forcing, (b) adiabatic forcing, (c) radiative forcing, (d) vertical diffusion and (e) total precipitation. Differences between high and low NAO composites are grey-shaded. The climatology forcing of the model, that is the average of the forcing over the winter season and all years, is also shown (contour lines are for ±0.1, ±0.25, ±0.5, ±0.75, ±1.0, ±1.5, ±2.5, ±4 $Kday^{-1}$; positive (negative) contours are solid (dashed)).

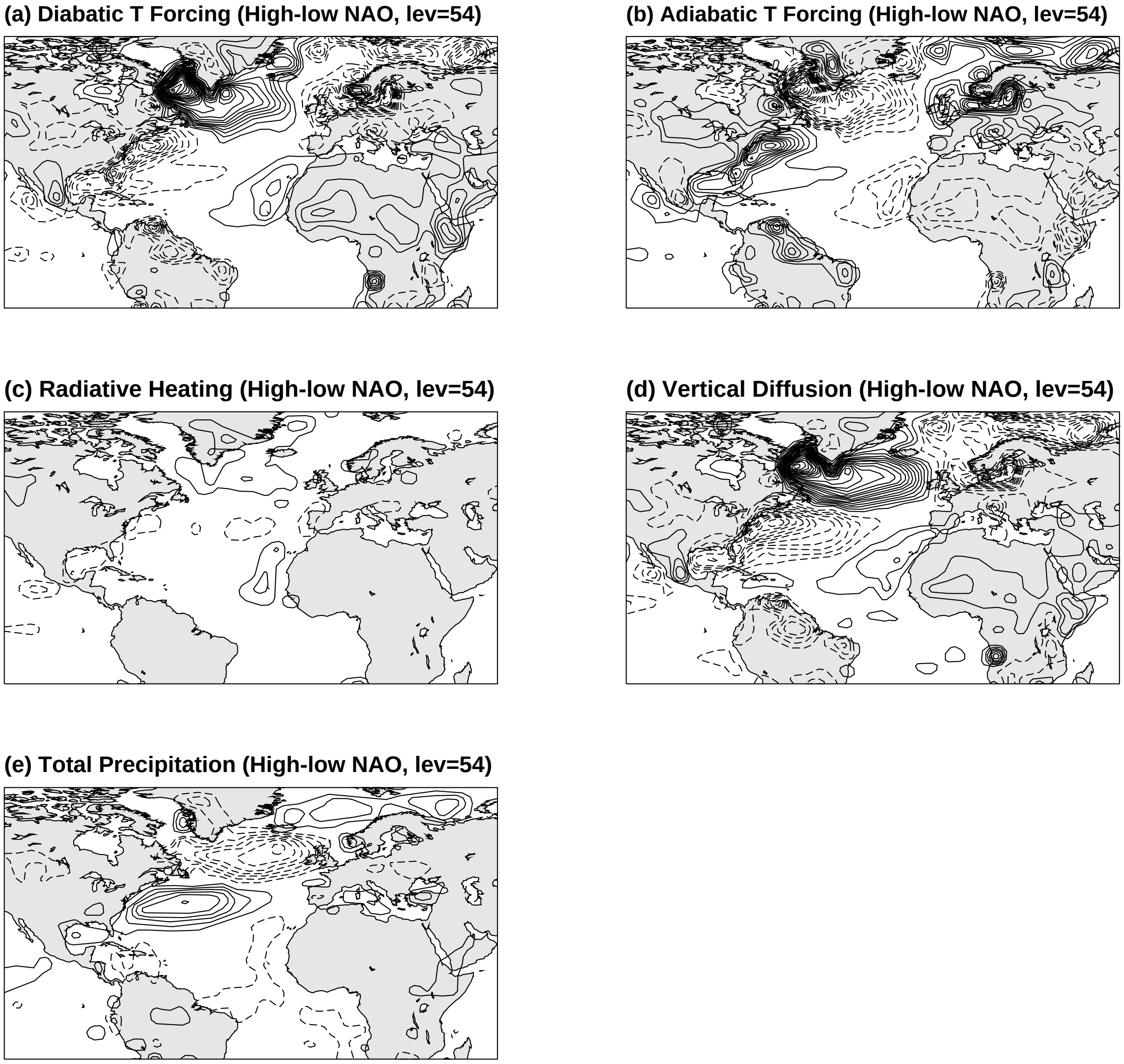

Figure 3. Mean difference of the temperature forcing at model level 54 (about 960 hPa) between high and low NAO composites (contour interval is $0.4\ K\ day^{-1}$) for the ECMWF model: (a) total diabatic forcing, (b) adiabatic forcing, (c) radiative forcing, (d) vertical diffusion, (e) total precipitation. The compositing technique is the same as that used to produce Figure 1. Positive (negative) contours are solid (dashed).

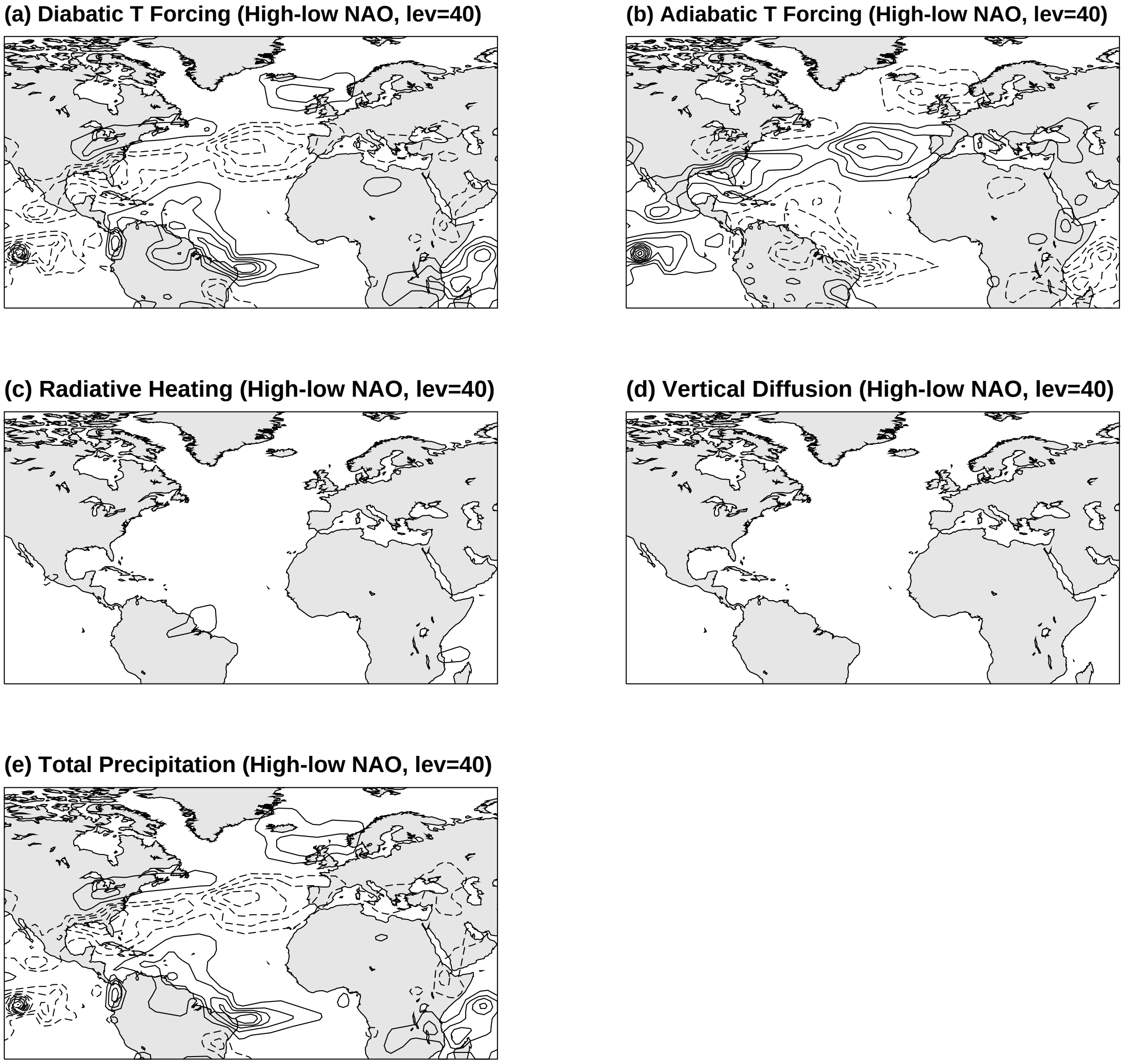

Figure 4. Same as Figure 3, except for model level 40 (about 540 hPa).

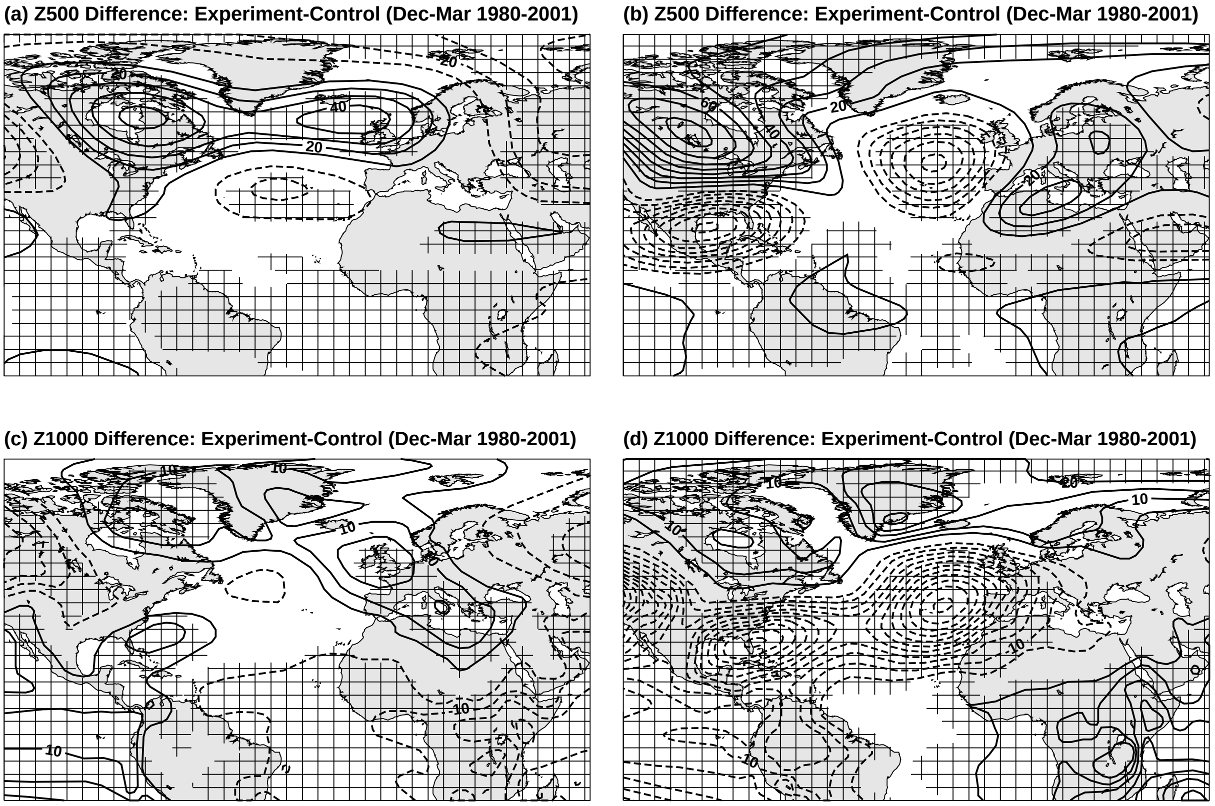

Figure 5. Difference of mean Z500 fields between an experiment with additional *global*, *total* diabatic forcing associated with the (a) positive and (b) negative phase of the NAO and a control integration with no additional forcing. (c) and (d) are the same as in (a) and (b), except for the 1000 hPa level (Z1000). Statistically significant differences which are at the 95 % confidence level are hashed.

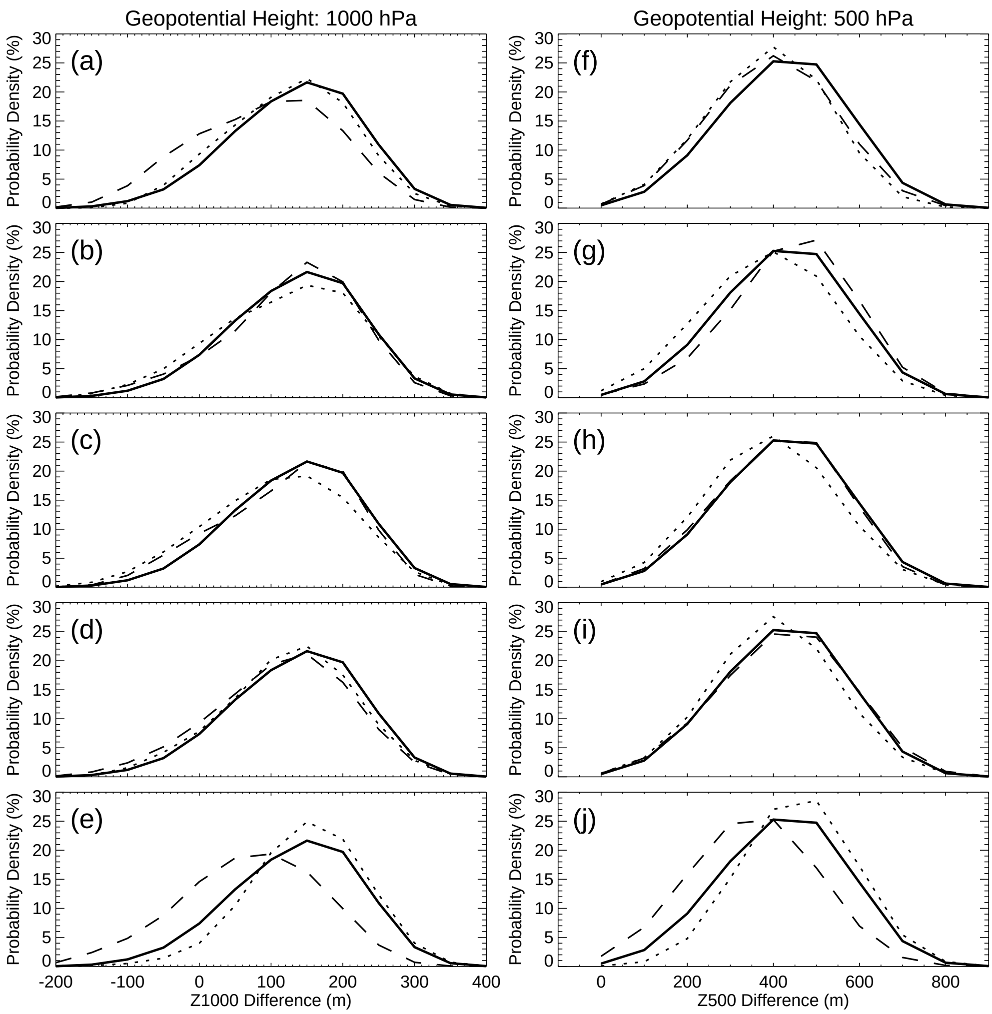

Figure 6. Probability density functions (pdf's) for the monthly mean difference in Z1000 (left column) and Z500 (right column), Azores minus Iceland, in metres. The solid lines show the control run in all cases. The dotted (dashed) lines show the experiments for diabatic forcings associate with the positive (negative) NAO. Pdf's for (a) and (f) global forcing, (b) and (g) North Atlantic forcing, (c) and (h) diffusion forcing, North Atlantic only, (d) and (i) precipitation forcing, North Atlantic only, and (e) and (f) tropical Pacific forcing. In order to describe the variations in the strength of the Azores high (Icelandic low), geopotential height fields were averaged over the area 0–60^{o}W, 35–45^{o}N (0–60^{o}W, 60–70^{o}N).

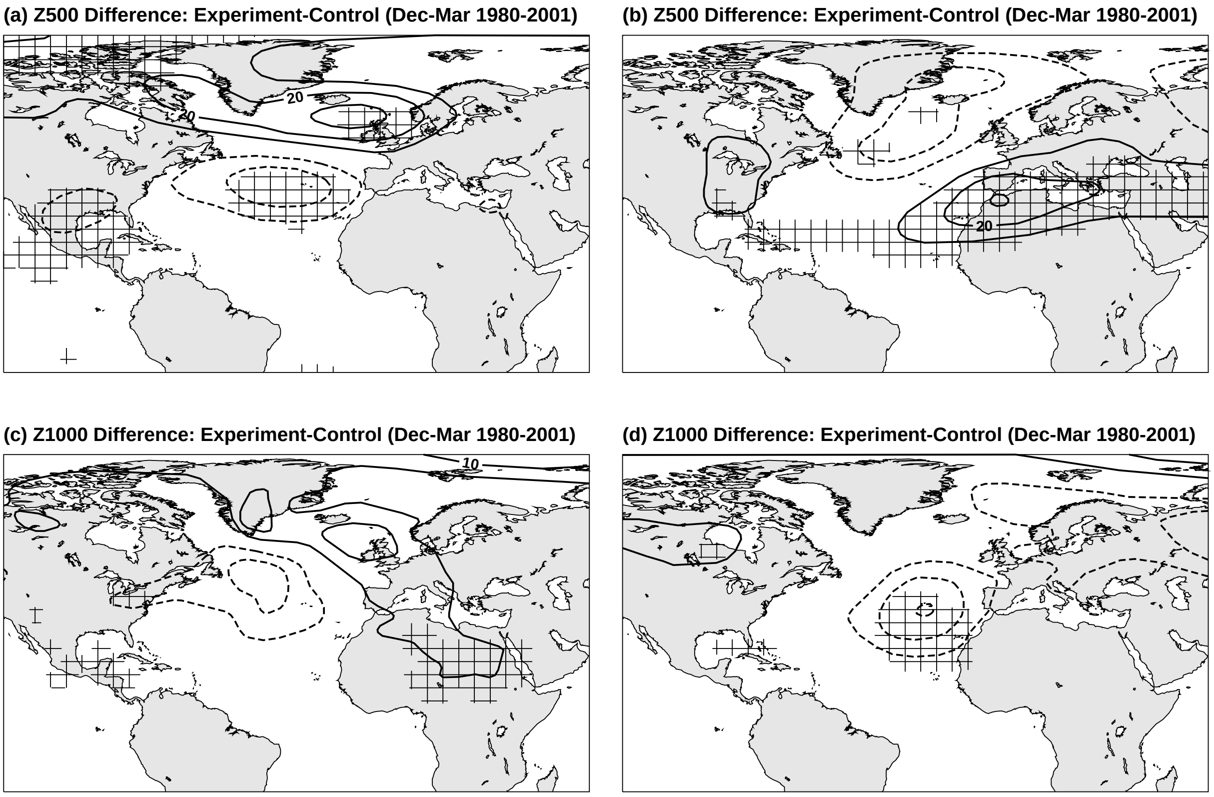

Figure 7. Same as in Figure 5, except for the NAO-related *total* diabatic forcing specified in the North Atlantic region only. (Diabatic forcing outside the area 100^{o}W–20^{o}E and 20–70^{o}N has been set to zero.)

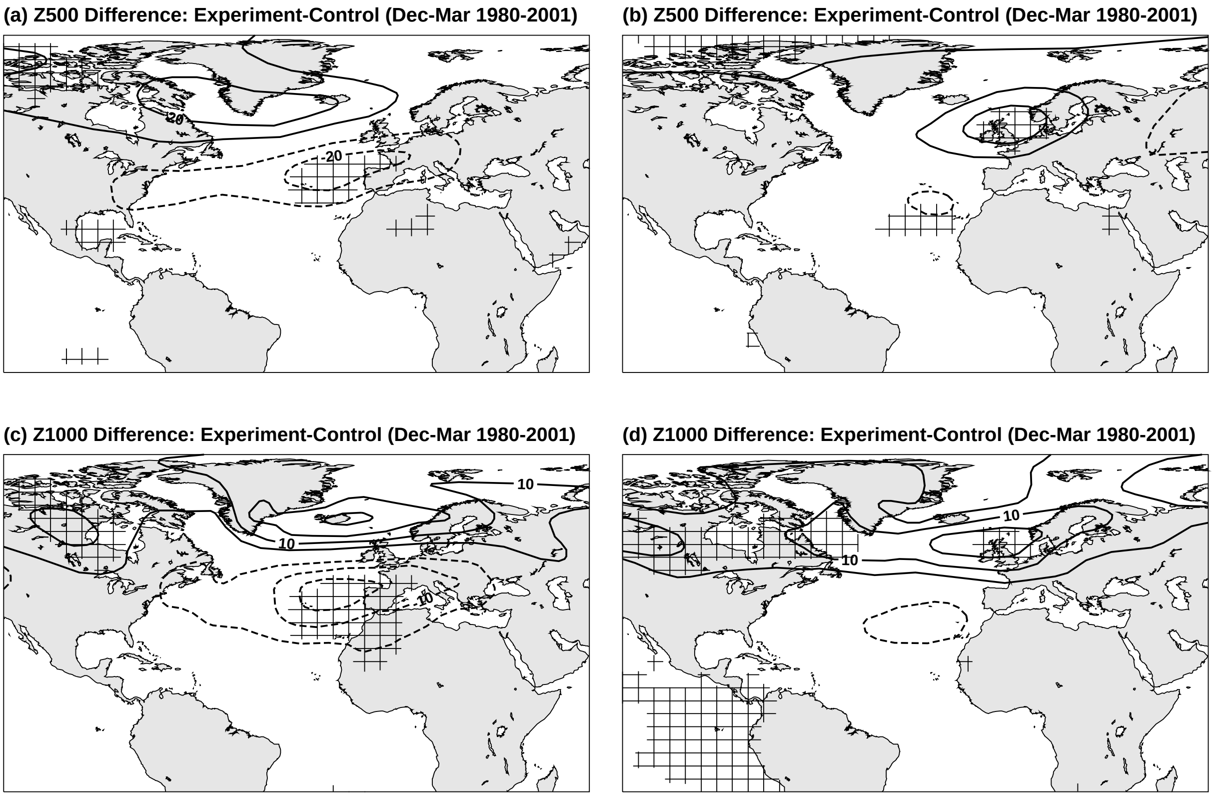

Figure 8. Same as in Figure 5, except for the NAO-related heating due to *diffusion* specified in the North Atlantic region only. (Diabatic forcing outside the area 100^oW–20^oE and 20–70^oN has been set to zero.)

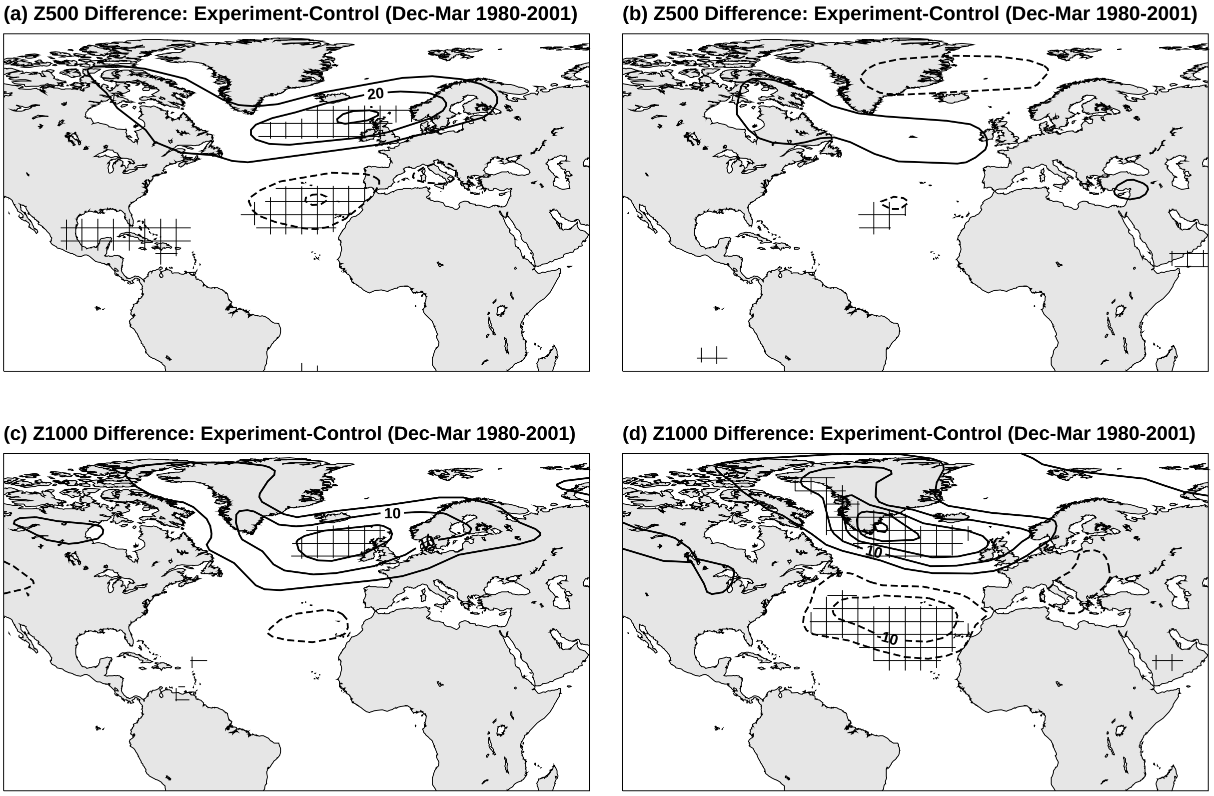

Figure 9. Same as in Figure 5, except for the NAO-related heating due to *precipitation* specified in the North Atlantic region only. (Diabatic forcing outside the area 100^oW–20^oE and 20–70^oN has been set to zero.)

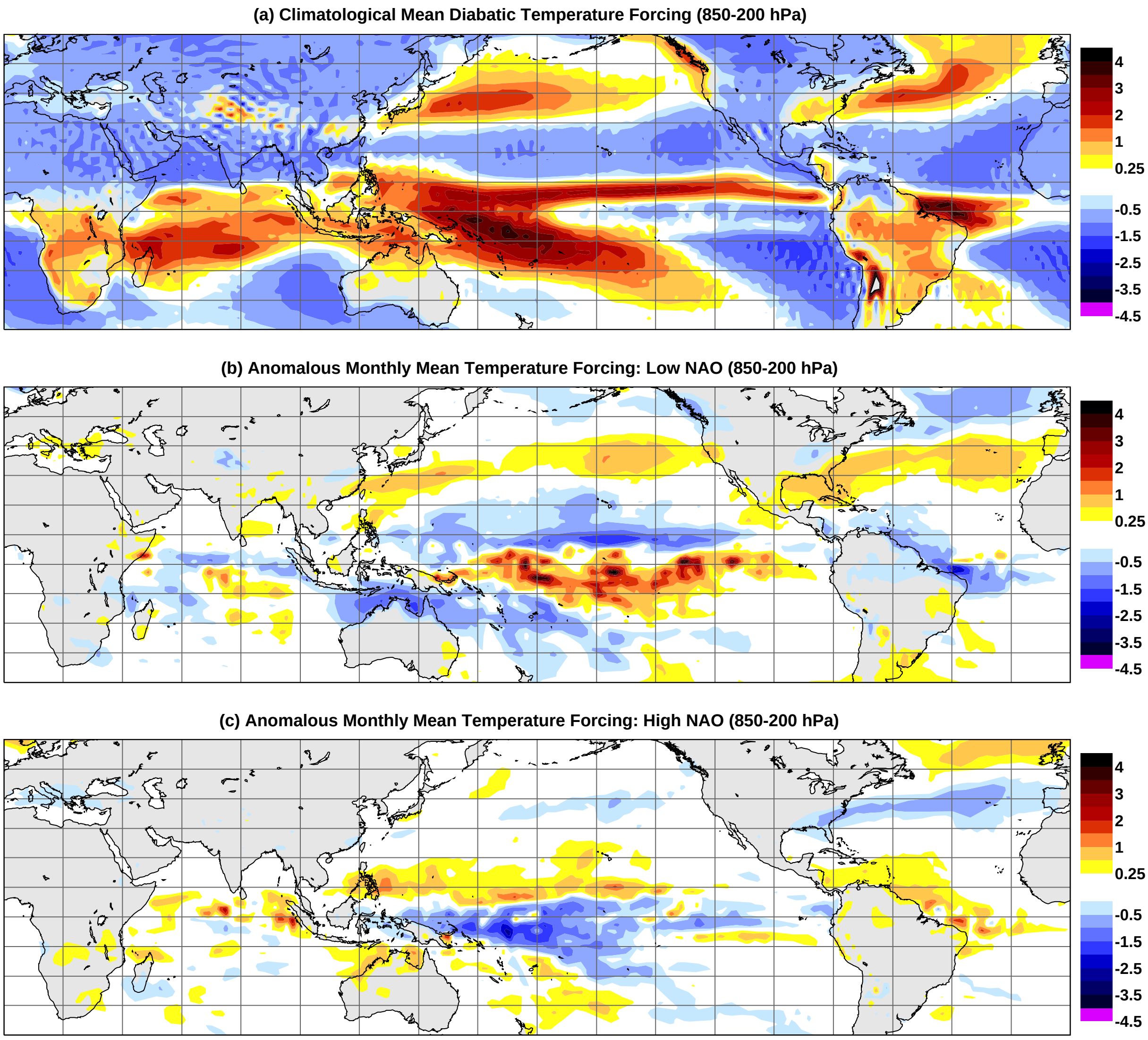

Figure 10. Diabatic heating (K/day) vertically integrated from 850–200 hPa: (a) Climatological mean values from the control integration. (b) Differences between *low* NAO months and climatological mean values. (c) Same as in (b), except for *high* NAO months.

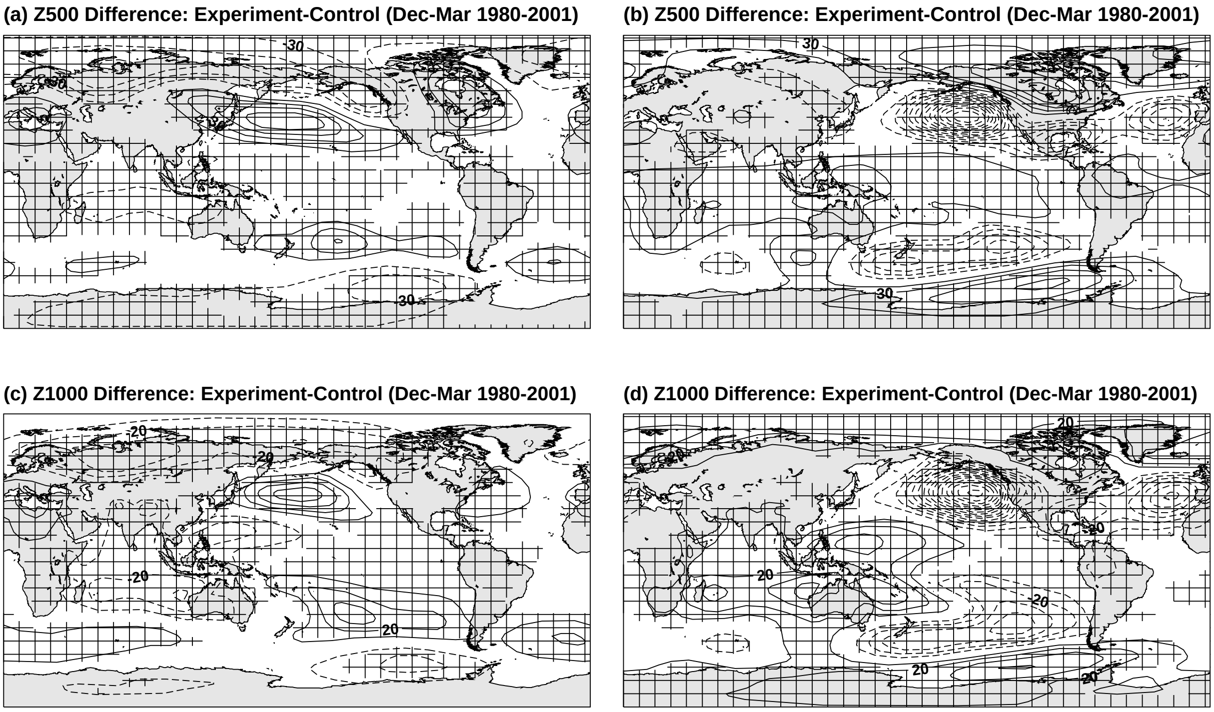

Figure 11. Same as in Figure 5, except for the NAO-related tropical heating due to *precipitation*. (Diabatic forcing outside the tropical Pacific, 20^{o}S–20^{o}N and 100^{o}E–100^{o}W, has been set to zero.)

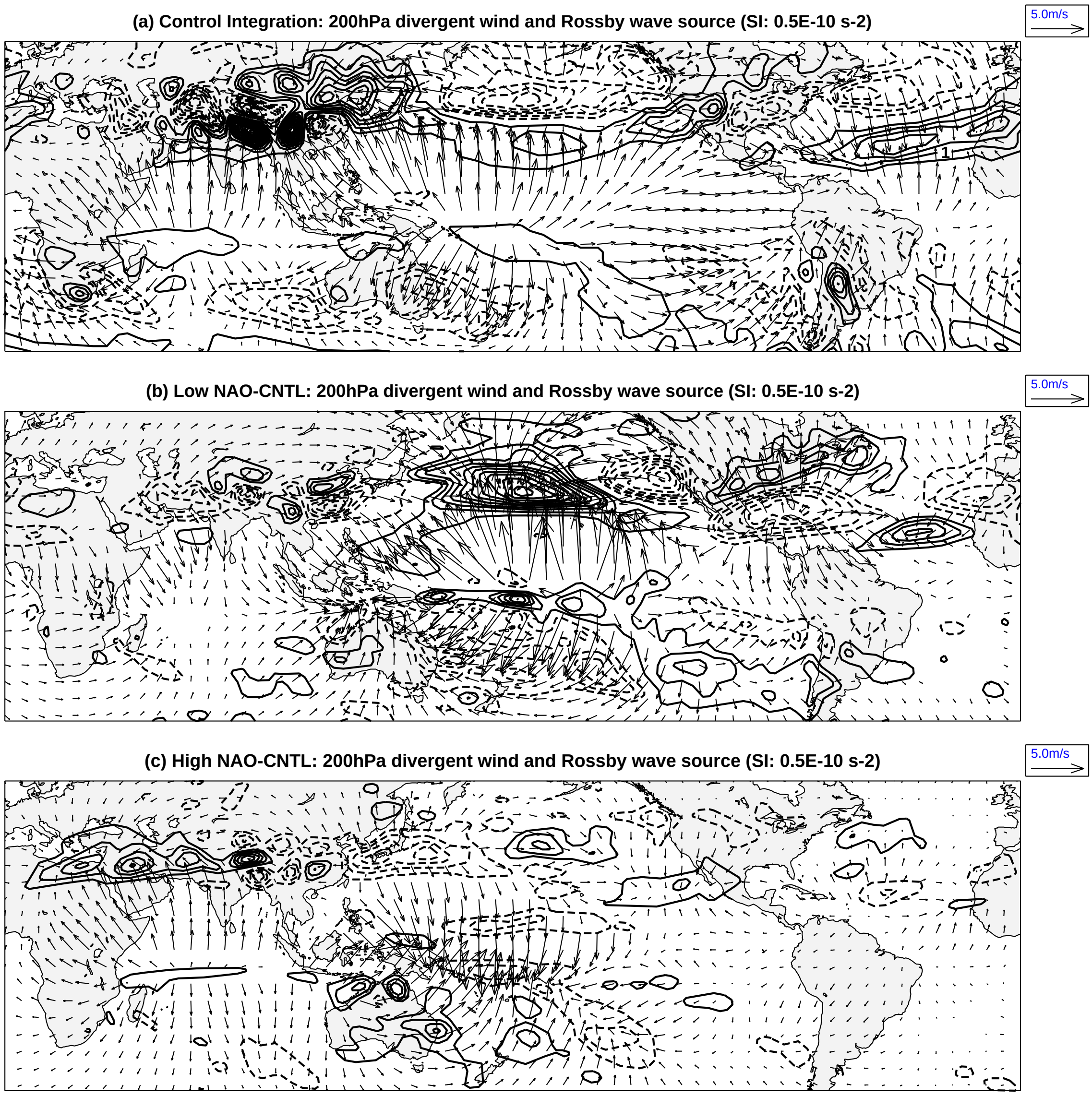

Figure 12. Divergent wind (m/s) and Rossby wave source (contour interval is $0.5 \cdot 10^{-10} s^{-2}$, negative values are dashed) at 200 hPa: (a) control integration, (b) difference between the sensitivity experiment with tropical diabatic temperature forcing due to precipitation associated with *low* NAO months and the control integration and (c) difference between the experiment with tropical diabatic temperature forcing due to precipitation associated with *high* NAO months and the control integration. A reference arrow for the divergent wind is given in the upper right corner of the graphs.